Proceedings of ISFOG 2025
5TH INTERNATIONAL SYMPOSIUM ON
FRONTIERS IN OFFSHORE GEOTECHNICS
Nantes, France | June 9-13 2025

ISBN 978-2-85782-758-0

3D DEM simulation of plain and rotary axial jacking of piles

B. Cerfontaine*
University of Southampton, Southampton, UK

M. Ciantia,
University of Dundee, Dundee, UK and Università degli Studi di Milano Bicocca, Milan, Italy

M.J. Brown, Y. Sharif
University of Dundee, Dundee, UK

D. White
University of Southampton, Southampton, UK

**b.cerfontaine@soton.ac.uk*

ABSTRACT: Increasingly stringent environmental regulations on underwater noise have led to the development of silent piling methods for offshore wind turbine foundations, such as plain axial jacking. However, the reaction force required for plain jacking equals the pile's axial compressive resistance, which may exceed the capabilities of offshore vessels. Rotary jacking, which involves pushing and rotating the piles, reduces the axial reaction force by rotating the shear stresses along the pile shaft and reducing pile plugging for open-ended piles. Despite its potential, the effects of rotary jacking on pile plugging are not well understood, hindering its development as an alternative to traditional pile driving. The discrete element method (DEM) simulates granular materials as assemblies of rigid particles, allowing for the simulation of large deformations during pile jacking. DEM also provides insights into the physical mechanisms within the ground, informing physical tests and guiding prediction methods. In this numerical study, an open-ended pile was subjected to both plain axial and rotary jacking in a polydisperse sample with upscaled particle diameters to reduce computational costs. Results indicated that rotary jacking reduced the necessary reaction force by 60%, due to (1) the rotation of the shear stress mobilised along the interface and (2) the reduction of pile plugging due to the disturbance created by the pile rotation. The coefficient of lateral earth pressure and the stress within the pile plug could be calculated and compared with the existing literature. These findings have significant implications for predicting the installation resistance and in-service capacity of rotary jacked piles.

Keywords: Pile; Silent piling; Rotary jacking; DEM

1 INTRODUCTION

Increasingly stringent environmental norms regulating underwater noise have led to the development of silent piling method to install offshore wind turbine foundations, as an alternative to pile driving. Pile jacking is a method that does not involve any impact, hence generates only a limited amount of noise (Igoe et al., 2013). It can be used to push clusters of piles that effectively replace large driven piles (Cerfontaine, Brown, et al., 2021; Huisman et al., 2022) However, the significant limitation of pile jacking for offshore applications is that the reaction force necessary during the pile installation must be equal to the pile compressive resistance, which may exceed the capacity of existing installation systems.

Rotary jacking, where a pile is both pushed and rotated about the vertical axis during its installation is an alternative jacking method that reduces the necessary vertical reaction force (Deeks et al., 2010; Ishihara et al., 2015). For instance, the "Gyro Piler" onshore technology has been developed by Giken in Japan, and demonstrates the feasibility of the concept (Hirata & Matsui, 2016). Deeks et al. (2010) and Sharif et al. (2021) have studied the effect of rotary-jacking on the pile penetration resistance for closed-ended piles, but only limited evidence exists for open-ended piles, especially on the plug formation during installation (Saathoff et al., 2020). The plugging process is particularly important for pile design, as it is intimately linked to the development of shaft resistance, as the radial stress existing along the outside and inside of the shaft depends on the plug length (Lehane et al., 2020).

The objective of this paper is to present a purely numerical study on rotary jacking of open-ended piles, with a particular focus on pile plugging, to inform future design guidelines. This is achieved by using the DEM (Discrete Element Method), which enables the analysis of local stresses acting along the pile or inside the plug, which is not available with the same detail and precision from standard field or lab tests.

2 DISCRETE ELEMENT MODEL

The DEM model, developed in PFC3D 6.00.17 (Itasca Consulting Group, 2019) is briefly introduced. For full details refer to Cerfontaine et al. (2023).

2.1 Calibration chamber

A 4.25m diameter and 10.5m high virtual calibration chamber was created to represent a centrifuge test environment with an enhanced gravity (model scaling factor = 50) (Figure 1). The soil domain was a dry polydisperse granular bed, whose particle size distribution is based on the HST95 sand available in Lauder (2010). The PSD was discretised by using 10 particle sizes (Figure 2). To reduce computational time, the particle diameters were upscaled by a scaling factor (SF) equal to 10.

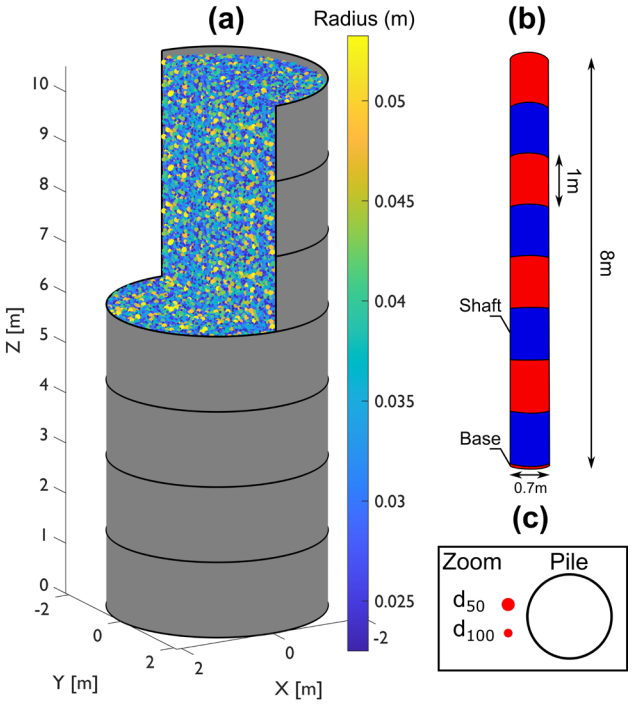

Figure 1 (a) Calibration chamber: particles and servo-controlled cylinders; (b) Model pile and its different components; (c) Comparison of upscaled particle sizes and pile diameter.

The sand bed was created by stacking seven representative elementary volumes (Ciantia et al., 2018). The target void ratio for the sand was set to 0.61, which corresponds to a relative density of 52% for the HST95. Seven servo-controlled cylinders, represented in Figure 1, were used to mimic a constant far-field stiffness and reduce the boundary effects created by the close proximity of the boundary. The procedure to calculate the constant stiffness associated with each cylinder is provided by Cerfontaine, et al. (2021), based on cylindrical cavity expansion and the shear modulus is given in Table 1.

Table 1 Shear moduli associated with each cylinder.

N	1	2	3	4	5	6	7
G [MPa]	4.3	7.8	10.3	12.4	14.2	15.9	17.4

2.2 Pile model

The open-ended pile was modelled as a rigid body with an external diameter equal to 0.7m and a wall thickness equal to 0.02m. The ratio of the wall thickness to the upscaled median particle dimension is equal to 0.28, which is lower than what is usually recommended for a sand in centrifuge testing to avoid scaling issues (Cerfontaine et al., 2023), but the use of smaller particles was computationally too expensive. The pile was installed by continuous jacking, which was imposed by fixing the vertical displacement rate (v_z) and the rotation rate (ω). The vertical rate was applied to ensure quasi-static conditions as per (Ciantia et al., 2019) and the rotation rate was calculated to impose an installation pitch (p_i),

$$p_i = \frac{\omega D}{2 v_z} \quad (1)$$

where D is the pile diameter. Two simulations were undertaken, one for which $p_i = 0$ (plain axial jacking) and one for which $p_i = 10$ (rotary jacking).

2.3 Contact model

The model used the Hertz-Mindlin relationship (Itasca Consulting Group, 2019), whose parameters are given in Table 1. The rotation of the spherical particles was prohibited to account for the non-sphericity of actual particles (Ting et al., 1989). A single set of parameters was calibrated by Sharif et al., (2019) against triaxial tests and is independent of the scaling factor applied to the particles, as the normal stiffness is calculated as a function of the particle size (Lommen et al., 2019), which preserves their properties for any representative elementary volume.

Table 2 Physical and model parameters after (Lauder, 2010; Y U Sharif et al., 2019).

Physical properties	
Minimum void ratio	0.467
Maximum void ratio	0.769
Critical state friction angle	32°
Median particle diameter (d_{50})	0.141mm
Maximum particle diameter (d_{max})	0.213mm
Minimum particle diameter (d_{min})	0.09mm
Coefficient of uniformity	1.9
DEM parameters	
Inter-particle shear modulus	3GPa
Poison's ratio	0.3
Inter-particle friction coefficient	0.264
Pile-particle friction coefficient	0.445
Cylinder-particle friction coefficient	0.8

The particle-pile friction coefficient depends on the pile roughness and the particle size and was estimated to be 0.445 by using a previous relationship (Ho et al., 2011) for the upscaled particles. The friction coefficient of the wall was set as 0.8 to reproduce a rough interface along the external walls.

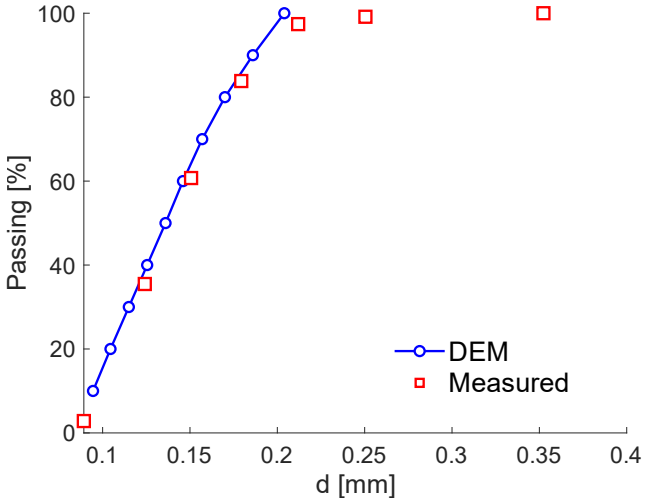

Figure 2 Particle size distribution as measured by (Lauder, 2010) *and discretised values used in the DEM model.*

3 RESULTS

3.1 Macroscopic results

As shown in Figure 2a, pile rotary jacking reduces the required vertical force by 60% at the end of the installation (8m depth, L/D =11.4) compared to plain axial jacking. This is caused by a ≥90% reduction in external shaft resistance and a 70% reduction in annular base resistance, as depicted in the figure. The mobilised friction inside the pile was only reduced by 20% and is not depicted here. The plug length is defined as the distance between the pile tip and the free surface of the soil inside the pile. A pile plugs when the plug length becomes significantly lower than the tip depth. Figure 2b shows that rotary jacking delays the plug formation when compared to plain axial jacking. Finally, the torque resistance during rotary jacking is depicted in Figure 2c and reaches a maximum of 2.7MNm. To contextualise this number, the Gyro Piler (GRV2540) of the Japanese company Giken can apply a torque of 2.9MNm, albeit to larger piles. This supports the fact that rotary installation is feasible in practice, though proper offshore tools would need to be developed.

3.2 Change in shear stress direction along the interface

As shown in Figure 3, the controlling mechanism underlying rotary jacking is that the orientation of the shear stress mobilised on the shaft (τ) is aligned with the velocity (v) at any point along the interface (Deeks et al., 2010). The circumferential velocity (v_θ) is simply the product of the rotation rate (ω) and the radius (D/2). Therefore, the ratio of the circumferential to the vertical velocities is

$$\frac{v_\theta}{v_z} = \frac{\omega D}{2v_z} = p_i \qquad (2)$$

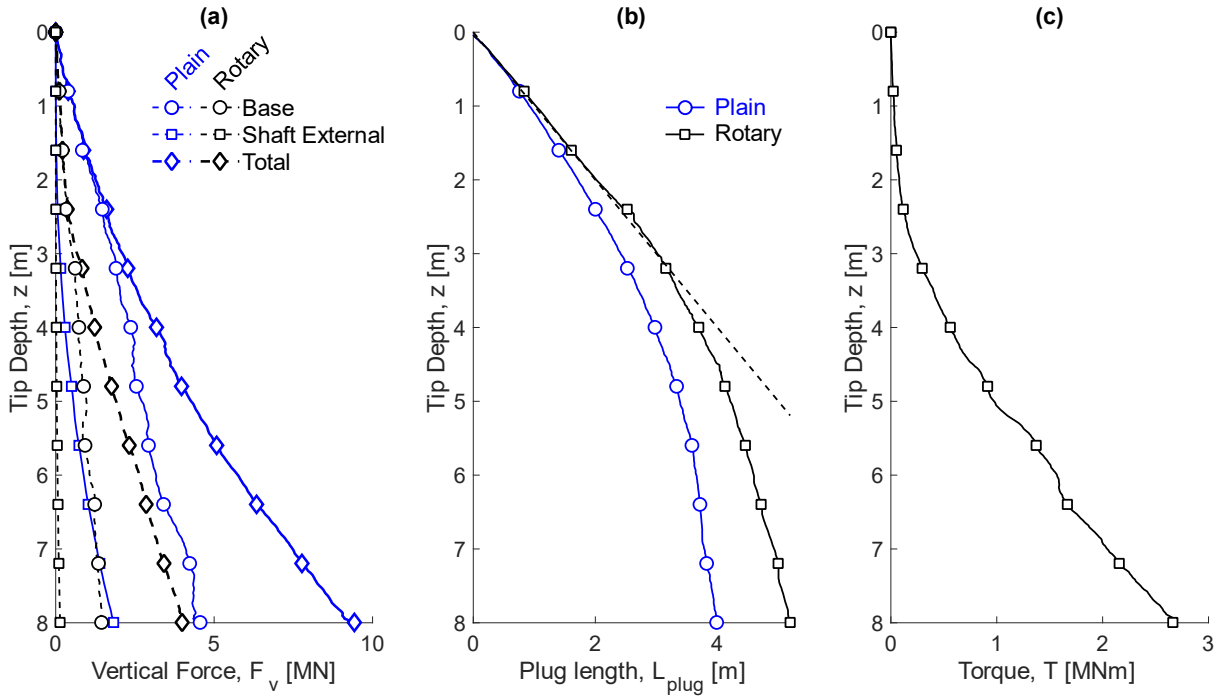

Figure 3 Variables measured during the pile installation: (a) Vertical force (Annular base, total external shaft, total force); (b) Plug length; (c) Torque (rotary jacking only). The origin of the z axis is at the soil surface.

The circumferential (τ_θ) and vertical (τ_z) components of the shear stress acting on the interface can then be calculated as

$$\tau_h = \frac{p_i}{\sqrt{1+p_i^2}}\tau \quad (3)$$

$$\tau_v = \frac{1}{\sqrt{1+p_i^2}}\tau \quad (4)$$

where τ is the mobilised shear stress. The vertical component (τ_v) will decrease with the installation pitch (p_i). The same equations can be applied on the inside and the outside of the pile.

A representation of the stress field at the pile-soil interface can be calculated by summing all contact forces acting on the shaft over a section of the pile and dividing the shaft surface area. For this work, fifteen 0.5m-high sections were selected, and an average shear or radial stress was calculated for each of them at the final stage of installation.

Rotary jacking causes a clear reduction in the magnitude of the vertical shear stress along the outside part of the shaft as shown in Figure 4a at the end of the installation (depth = 8m). For rotary jacking, the vertical component of shear stress is reduced to 3-7% of the plain axial jacking value. This reduction cannot be attributed only to the rotation of the shear stress direction, as calculated from Equation (4), assuming the same maximum shear resistance (τ) can be mobilised. However, the ratio of the orthoradial shear stress (τ_θ) to the vertical shear stress (τ_v) along most of the shaft is equal to 10, matching the installation pitch (Figure 4b), as expected. Therefore, the larger reduction in the mobilised friction is due to a reduced magnitude of radial stress on the pile, hence a reduced maximum mobilised friction. Figure 4b shows the ratio of the radial stress for plain axial compared to rotary jacking. This ratio exceeds one throughout the pile length, except within 2m from the tip, indicating a reduction in radial stress with rotary jacking. Since the rotary jacking proceeds with reduced plugging, there is a lower radial displacement of soil during the pile installation, created a lower radial stress on the shaft.

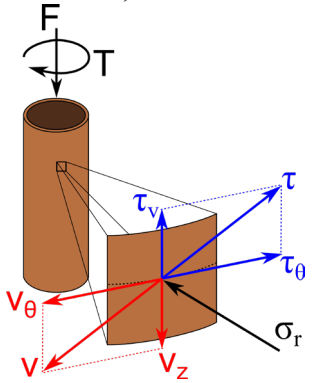

Figure 4 Stress state and velocity diagram at the pile-soil interface.

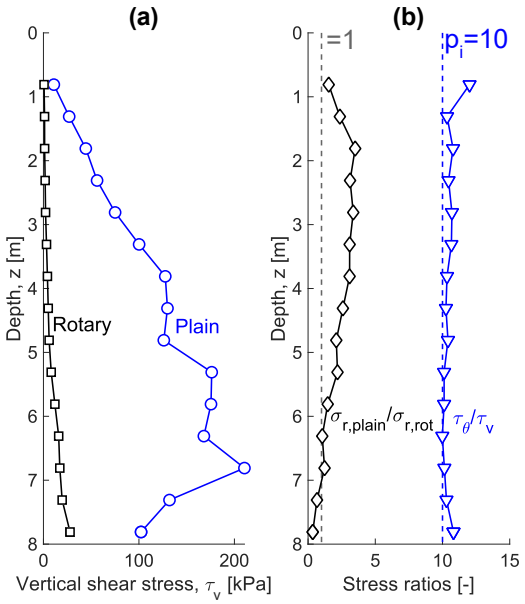

Figure 5 Distributions of stress along the pile shaft at the end of the installation for plain axial and rotary jacking: (a) Vertical shear stress; (b) Ratio of the radial stress in both cases and ratio of circumferential to vertical shear stress for rotary jacking.

The inclination of the shear stress mobilised along the shaft will always align with the movement direction of the pile, so the shear stress can be fully mobilised in tension. However, the lower radial stress created by rotary jacking, in contrast to plain jacking, means that a lower shaft capacity can be mobilised.

3.2.1 Soil deformation

The difference in plugging mechanism is evident in Figure 5, which shows the final displacement of particles around and inside the pile at the end of installation for plain axial and rotary jacking. The particles were coloured yellow or blue according to their initial position in the undisturbed sample, to display a layered pattern. The disturbance in each layer then becomes apparent after the installation of the pile.

The plug length is longer for the rotary case (Figure 5b) than for the plain case (Figure 5a) but also exhibits more disturbance. The plug layers exhibits chevron shapes, probably formed during the coring period of the pile. In contrast, plain axial jacking creates an alternated layering of the soil plug, where bands tend to be reduced in thickness as the pile tends towards full plugging and material is diverted around the pile shaft.

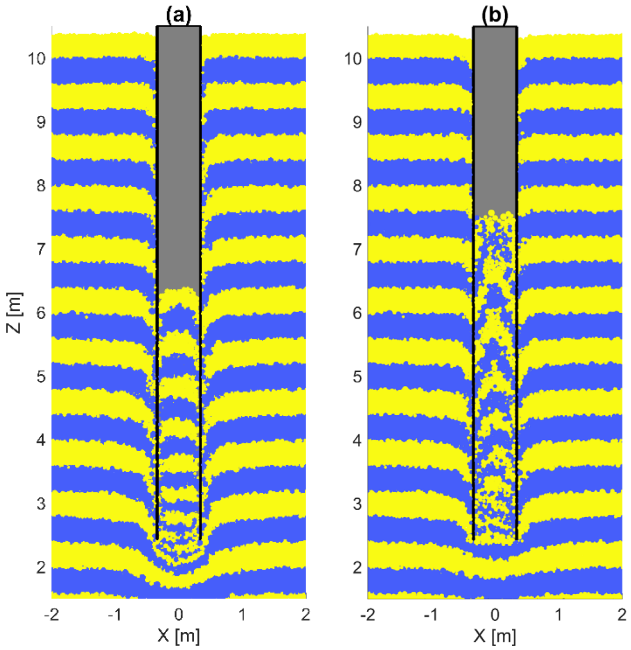

Figure 6 Particle distributions around the pile and in the pile plug at the end of installation for (a) plain axial jacking and (b) rotary jacking.

The reduced base penetration resistance observed in Figure 2 can be linked to the different deformation mechanism under the pile tip. The plain axial jacking creates a "shield" (= arching) underneath the tip that deforms the soil layers more than one meter in advance of the tip. This effect is almost not visible for the rotary jacking case.

3.2.2 Stress field

Figure 6 compares the stress field within the plug for plain axial and rotary jacking. The radial stress within the plug was calculated in two different, but convergent, ways in Figure 6a: 1) by integrating all contact forces along the interface and 2) by calculating the average stress between the particles in and below the plug volume. The stress state within the volume of the plug is probably less uniform or more complex than at the interface, hence the difference between the two methods. The results show that rotary jacking incudes a greater radial stress on the inside of the plug. This may seem counter-intuitive as the plug length is longer for the rotary jacked case, but could be explained by two phenomena. Firstly, the rotation of principal stresses also takes place along the internal interface, which reduces the vertical resistance to sliding of the plug. Secondly, the rotary movement strongly interferes with interparticle force chain development underneath the pile. In the plain jacking case, arching force chains reacting against the pile annular base are created and "shield" the stress acting at the bottom of the plug (see also Figure 5). The rotary movement destabilises those chains, which increases the vertical and radial stresses acting on the plug. This is illustrated in Figure 7, which shows that the ratio of normal stress acting on the annular pile tip to the normal stress acting on the plug is lower in the case of rotary jacking.

Figure 6b shows the average radial to vertical stress calculated within the soil plug in both cases. This value

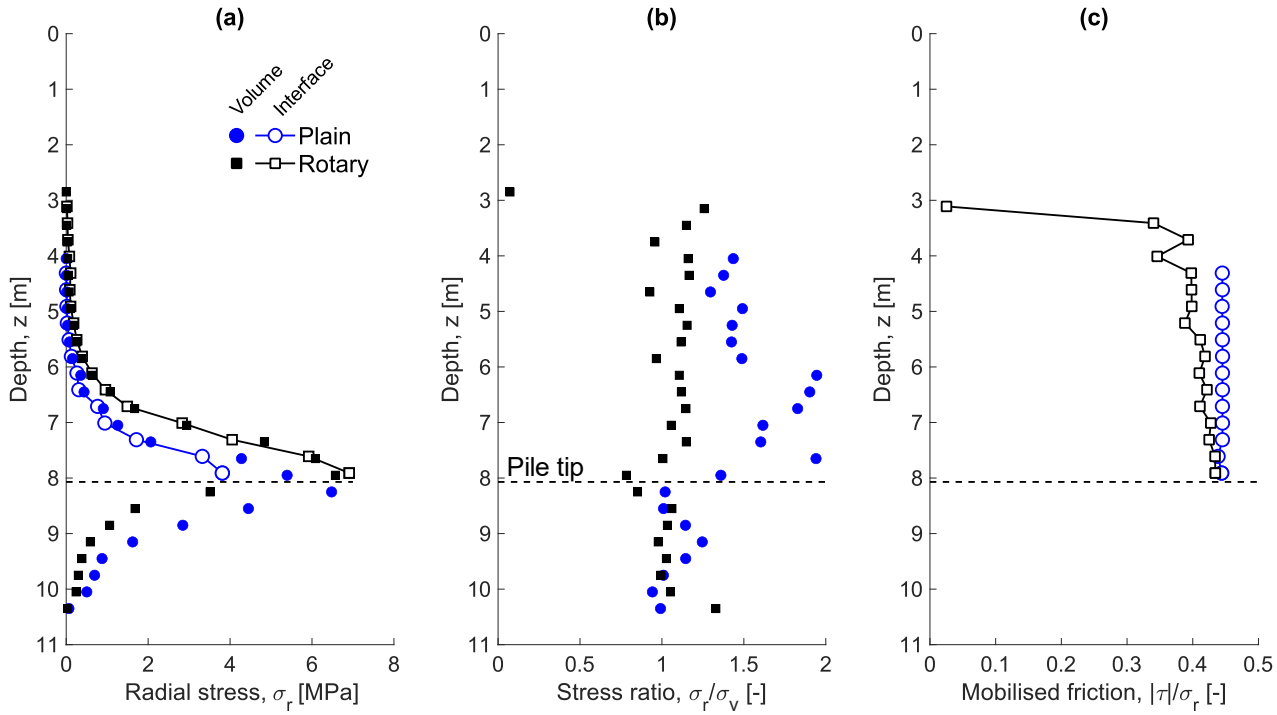

Figure 7 Stress state within the plug and at the plug-pile interface for plain and rotary jacking: (a) Radial stress; (b) Radial to vertical stress ratio; (c) Mobilised friction at the interface. Data were averaged over 0.3m high intervals.

is often assumed, rather than measured, as it is particularly complicated to instrument a full-scale pile to differentiate between external and internal loads (Igoe & Gavin, 2010). The results show a fairly constant ratio across the height of the plug in the case of rotary jacking (~1.15) and a variable ratio for plain jacking (1.4-1.95). This is larger than the coefficients determined through centrifuge modelling (De Nicola & Randolph, 1997) for plain jacking (≤1) and there are no comparison points in the literature for rotary jacking.

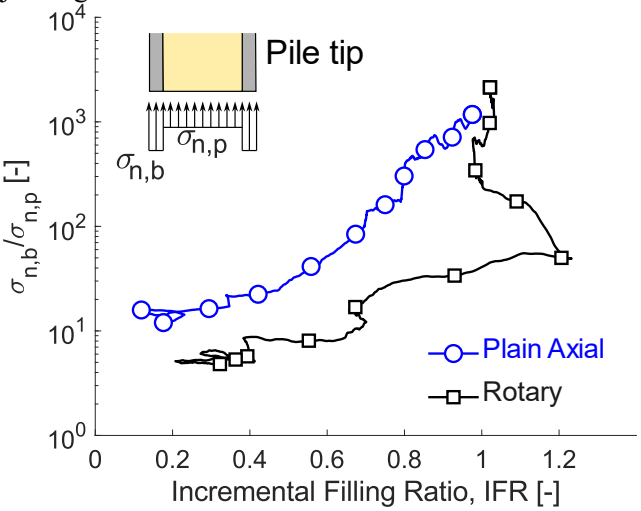

Figure 8 Ratio of the average vertical normal stress on the annular tip of the pile to the average vertical normal stress acting on the base of the pile plug, as a function of the internal filling ratio (IFR): plugging (IFR = 0).

Finally, Figure 6c shows the mobilised total shear stress (τ) along the inner wall of the pile at the end of installation. For plain jacking, the mobilised friction is almost equal everywhere to the assigned friction coefficient, while it is lower for rotary jacking. This means that the plug is not in a coring phase. Further inspection of the particle displacement inside the plug shows that it is rotating with the pile.

The results given in Figure 6 are a snapshot at a given time step, and for the modelled conditions. For instance, no volume reduction due to particle crushing was modelled, yet this phenomenon occurs at high vertical stress and strain near a pile tip (White & Bolton, 2004). However, the results presented in this section have the potential to inform existing models or experimental results by revealing more of the micromechanical mechanisms taking place during plugging. They also offer insights into how pile installation resistance may be reduced to aid quieter deployment or easier driving.

3.3 Particle scaling

The upscaled particles used in this work are representative of cobbles at prototype scale, though the properties assigned to the soil mass are those of a sand. It was shown by Cerfontaine et al. (2023), that using larger particles leads to earlier plugging, enhanced lateral soil displacement during installation and ultimately to greater radial stress along the outer shaft. It was also shown that the main particle scaling issues for small scale models were related to the pile wall thickness to median particle size diameter ratio (t/d50), which affects the coring mechanism and the transition to a fully plugged section, rather than to the pile outer diameter to median particle size diameter (D/d_{50}). This latter ratio is equal to 10 in this study. This is lower than what would be expected in a physical model such as centrifuge testing (Garnier et al., 2007), but is almost twice the ratio used in past studies on cone penetration (Ciantia et al., 2019), which were validated against experimental data.

4 CONCLUSIONS

DEM simulations were undertaken to study plain axial and rotary jacking of a straight-shafted short pile, as a silent installation alternative to driven piles. Results show that rotary jacking can reduce the reaction force necessary for installation by 60% in a granular material with the properties of a sand. This reduction comes from a reduction in base and shaft penetration resistance due to two main mechanisms. Firstly, the mobilised shear stress acting along the soil-pile interface aligns with the velocity of surface of the rotating pile, which reduces the vertical shaft resistance and creates a torque resistance. Secondly, the pile rotation increases the plug length by reducing the inner wall friction, but also by destabilising any arching or shielding that usually develops from the pile annular tip during plain jacking. Consequently, it was shown that the radial stress along the external shaft is lower for rotary than for plain axial jacking, which could have consequences for the subsequent in-service design of the pile tensile capacity. The DEM simulation also offers the possibility to interrogate the stress field and displacement pattern in the plug and calculate the lateral earth coefficient, which is often an assumed parameter in simplified models. The results showed that this coefficient was larger than expected in the literature, though the absence of particle rolling and grain crushing could affect those results. Further experimental results are necessary to validate the numerical results, especially the plug behaviour.

AUTHOR CONTRIBUTION STATEMENT

B. Cerfontaine: Conceptualization, Methodology, Formal Analysis, Writing- Original draft. **M. Ciantia**: Software, Methodology. **M. Brown**: Methodology,

Writing – review & editing, Supervision, Funding acquisition. **Y. Sharif and D. White**: Writing-Reviewing and Editing,

REFERENCES

Cerfontaine, B., Brown, M. J., Ciantia, M., Huisman, M., & Ottolini, M. (2021). Discrete element modelling of silent piling group installation for offshore wind turbine foundations. *Proceedings of the Second International Conference on Press-in Engineering*.

Cerfontaine, B., Ciantia, M., Brown, M. J., & Sharif, Y. U. (2021). Computers and Geotechnics DEM study of particle scale and penetration rate on the installation mechanisms of screw piles in sand. *Computers and Geotechnics*, *139*, 104380. https://doi.org/10.1016/j.compgeo.2021.104380

Cerfontaine, B., Ciantia, M. O., Brown, M. J., White, D. J., & Sharif, Y. U. (2023). DEM study of particle scale effect on plain and rotary jacked pile behaviour in granular materials. *Computers and Geotechnics*, *161*(May), 105559. https://doi.org/10.1016/j.compgeo.2023.105559

Ciantia, M. O., Boschi, K., Shire, T., & Emam, S. (2018). Numerical techniques for fast generation of large discrete-element models. *Proceedings of the Institution of Civil Engineers: Engineering and Computational Mechanics*, *171*(4), 147–161. https://doi.org/10.1680/jencm.18.00025

Ciantia, M. O., O'Sullivan, C., & Jardine, R. J. (2019). Pile penetration in crushable soils : Insights from micromechanical modelling. *Proceedings of the XVII ECSMGE-2019*, *September*, 298–317. https://doi.org/10.32075/17ECSMGE-2019-1111

De Nicola, A., & Randolph, M. F. (1997). The plugging behaviour of driven and jacked piles in sand. *Geotechnique*, *47*(4), 841–856. https://doi.org/10.1680/geot.1997.47.4.841

Deeks, A. D., White, D. J., & Ishihara, Y. (2010). Novel piling:Axial and rotary jacking. *Conference of the Deep Foundation Institute*, *May*, 24.

Garnier, J., Gaudin, C., Springman, S. M., Culligan, P. J., Goodings, D., Konig, D., Phillips, R., Randolph, M. F., & Thorel, L. (2007). Catalogue of scaling laws and similitude questions in geotechnical centrifuge modelling. *International Journal of Physical Modelling in Geotechnics*, *3*, 1–23.

Hirata, H., & Matsui, N. (2016). *Expanding Applications of the Gyropress Method ™* (Issue 113).

Ho, T. Y. K., Jardine, R. J., & Anh-Minh, N. (2011). Large-displacement interface shear between steel and granular media. *Geotechnique*, *61*(3), 221–234. https://doi.org/10.1680/geot.8.P.086

Huisman, M., Ottolini, M., Cerfontaine, B., Brown, M. J., Davidson, C., & Sharif, Y.]Robinson, S. (2022). Design Optimisation of Deep Pile Foundations Installed by Static Forces. *Proceedings of the Offshore Technology Conference Asia, OTC Asia*. https://doi.org/https://doi.org/10.4043/31461-MS

Igoe, D., Gavin, K., & O'Kelly, B. (2013). An investigation into the use of push-in pile foundations by the offshore wind sector_International Journal of Environmental Studies. *International Journal of Environmental Studies*, *70*(5), 777–791.

Igoe, D., & Gavin, P. K. (2010). The development and testing of an instrumented Open-Ended model pile. *Geotechnicla Testing Journal*, *33*(1), 3–14. https://doi.org/10.1520/GTJ102708

Ishihara, Y., Haigh, S., & Bolton, M. (2015). Estimating base resistance and N value in rotary press-in. *Soils and Foundations*, *55*(4), 788–797. https://doi.org/10.1016/j.sandf.2015.06.011

Itasca Consulting Group. (2019). *PFC3D 6.17*.

Lauder, K. (2010). *The performance of pipeline ploughs*. PhD thesis, University of Dundee, UK.

Lehane, B., Liu, Z., Bittar, E., Farrokh, N., Lacasse, S., Jardine, R., Carotenuto, P., Rattley, M., & Gavin, K. (2020). A new "unified" CPT-based axial pile capacity design method for driven piles in sand. *Fourth International Symposium on Frontiers in Offshore Geotechnics*, 462–477.

Lommen, S., Mohajeri, M., Lodewijks, G., & Schott, D. (2019). DEM particle upscaling for large-scale bulk handling equipment and material interaction. *Powder Technology*, *352*, 273–282. https://doi.org/10.1016/j.powtec.2019.04.034

Saathoff, J. E., Frick, D., & Achmus, M. (2020). *Chapter ROTARY-JACKED Waste dumps – tips , tailings and lagoons*. 241–246.

Sharif, Y U, Brown, M. J., Ciantia, M. O., Knappett, J. A., Davidson, C., Cerfontaine, B., & Robinson, S. (2019). Numerically modelling the installation and loading of screw piles using DEM. *1st International Symposium on Screw Piles for Energy Applications*, *May 2019*, 27–28.

Sharif, Yaseen Umar, Brown, M. J., Ciantia, M. O., Cerfontaine, B., Davidson, C., Knappett, J., Meijer, G. J., & Ball, J. (2021). Using discrete element method (DEM) to create a cone penetration test (cpt)-based method to estimate the installation requirements of rotary-installed piles in sand. *Canadian Geotechnical Journal*, *58*(7), 919–935. https://doi.org/10.1139/cgj-2020-0017

Ting, J. M., Corkum, B. T., Kauffman, C. R., & Greco, C. (1989). Discrete Numerical Model for Soil Mechanics. *Journal of Geotechnical Engineering*, *115*(3), 379–398.

White, D. J., & Bolton, M. D. (2004). Displacement and strain paths during plane-strain model pile installation in sand. *Géotechnique*, *54*(6), 375–397.